Original Article

INFECTIOUS Microbes & Diseases

OPEN

Protection Against Lethal Multidrug-Resistant Bacterial Infections Using Macrophage Cell Therapy

Robert Tacke[1,#], Josh Sun[1,2,3,4,#], Satoshi Uchiyama[2,3], Anya Polovina[1], Deborah G. Nguyen[1,✉], Victor Nizet[2,3,4,✉]

Abstract

Multidrug-resistant (MDR) bacterial infections exert a tremendous burden on the public health system throughout the developing and developed world. Slowing development of novel antibiotic scaffolds, over-prescription of antibiotics, extensive agricultural antibiotic use, and the increasingly complex hospitalized patient populations undergoing treatment, all fuel the rise of highly MDR "superbugs." Unfortunately, host-directed therapies to boost immune resistance to infection are not currently available for treatment of MDR pathogens. Hematopoietic cells are endowed with a variety of mechanisms to control microbial invasion. Macrophages in particular have long been appreciated as potent antimicrobial immune cells equipped with several receptors that allow for rapid recognition, phagocytosis, and killing of pathogenic microbes, coupled to secretion of immunostimulatory cytokines to further orchestrate a robust multifaceted antibacterial immune response. To investigate the utility of macrophages as a cell therapy for MDR bacterial infections, we developed a therapeutically translatable process to generate, harvest, and cryopreserve monocyte-derived macrophages (ICONIMAC™). These cells effectively killed both Gram-positive and Gram-negative MDR pathogens in vitro, and conferred protection in vivo against experimental lethal peritonitis and lung infection. Our discoveries provide a proof-of-concept for a novel immunotherapeutic approach against MDR bacterial infections, urgently needed to supplement the diminishing antibiotic pipeline.

Keywords: antibiotic resistance; innate immunity; bacterial infection; macrophage; cell therapy; ICONIMAC™; *Staphylococcus aureus*; *Pseudomonas aeruginosa*; *Klebsiella pneumoniae*

Introduction

Decades of antibiotic overuse, an innovation gap in this sector of pharmaceutical development, and the continual evolution of drug-resistant strains have led to dangerous increases in morbidity, mortality, and healthcare costs associated with serious bacterial infections. In the United States alone, it is estimated that more than 2.8 million people acquire a drug-resistant bacterial infection each year, with up to 162,000 deaths, $20 billion in added healthcare costs and $35 billion in lost productivity.[1,2] Hospitalization is a major risk factor for bacterial infections, which are acquired by up to 50% of intensive care unit patients, markedly increasing their length of stay and mortality risk.[3] New antibacterial agents are being developed to combat complicated infections, but most display similar mechanisms of action (MOA) as existing antibiotics, limiting their spectrum to a subset of pathogens and making future resistance evolution inevitable.[4] For these reasons, there is a critical need for broad-spectrum antibacterial therapeutic modalities with lower resistance and toxicity profiles.

The innate immune system evolved as a broad-spectrum, pathogen-agnostic defense system that protects us against the large array of potential pathogens we encounter in our environment. Proper functioning of innate immunity plays a pivotal role in eradicating pathogenic bacteria from the body in combination with source control and antibiotic therapy. However, age, underlying disease, or drug treatment can reduce efficacy of the innate immune system, rendering the host immunocompromised and increasing the risk of treatment failure.[5–7] Strategies designed to augment the host innate immune system would be a powerful adjunct to the existing standard of care (SOC).

Macrophages are linchpins of the innate immune system, rapidly engulfing and destroying pathogens, releasing factors that attract and stimulate other immune cells, and then cleaning up residual debris to restore baseline homeostatic functions.[8,9] It has been demonstrated that macrophages in culture can kill a variety of different bacterial strains including those with drug-

Editor: Stijn van der Veen

[1] Cellular Approaches, San Diego CA, 92037, USA, [2] Collaborative to Halt Antibiotic-Resistant Microbes (CHARM), UC San Diego, La Jolla, CA 92093, USA, [3] Department of Pediatrics, UC San Diego, La Jolla, CA 92093, USA, [4] Skaggs School of Pharmacy and Pharmaceutical Sciences, UC San Diego, La Jolla, CA 92093, USA.

✉Corresponding authors: Deborah G. Nguyen, Cellular Approaches, 11099 North Torrey Pines Road, Suite 290, San Diego, CA 92037, USA. E-mail: dnguyen@cellularapproaches.com; Victor Nizet, Collaborative to Halt Antibiotic-Resistant Microbes (CHARM), Department of Pediatrics, UC San Diego, 9500 Gilman Drive Mail Code 0760, La Jolla, CA 92093, USA. E-mail: vnizet@ucsd.edu

[#]Robert Tacke and Josh Sun contributed equally.

Author Contributions: RT, JS, SU, DN, and VN designed the research; RT, JS, SU, and AP performed the research; RT, JS, SU, AP, DN, and VN analyzed the data; RT, JS, DN, and VN wrote the manuscript, with all authors providing critical review and feedback.

Funding: Research was funded by Cellular Approaches, Inc.

Conflicts of Interest: RT, JS, AP, and DN are employees of Cellular Approaches, Inc. Studies at UC San Diego were supported by a sponsored research agreement with Cellular Approaches, Inc. VN previously received fees as a consultant for Cellular Approaches, Inc.

Infectious Microbes & Diseases (2019) 1:2

Received: 3 October 2019 / Received in final form: 23 October 2019 / Accepted: 28 October 2019

http://dx.doi.org/10.1097/IM9.0000000000000012

resistance.[10–12] In addition to direct bacterial killing, binding of bacteria to the macrophage surface activates a signaling cascade that results in the production of immunostimulatory cytokines that recruit other immune cells to the site of infection.[9,13] Together, this combination of direct bacterial cell killing and indirect immune cell recruitment enhances the effective clearance of bacterial infections.[14] Considering that macrophages evolved to quickly defend the host against a diverse array of bacterial, fungal and viral species, we developed a monocyte-derived macrophage cell therapy (ICONIMAC™) as a complementary adjunctive therapy with the necessary adaptive breadth of antimicrobial responses to improve infection outcomes *via* a mechanism independent of most common bacterial resistance pathways.

Here we demonstrate that ICONIMAC™ can be generated through a simple and good manufacturing practice (GMP) compatible process, in which cells can be cryopreserved and delivered "off the shelf." Both allogeneic and xenobiotic ICONIMAC™ macrophages rescued immune-competent mice from infection-induced lethality, without inducing an excessive inflammatory response or graft versus host disease (GVHD). Data from this study support the continued development of macrophage-based cell therapy strategies to treat antibiotic-resistant bacterial infections.

Results

Previous studies have demonstrated that cultured macrophages kill bacteria and that treatment with interferon-γ (IFNγ) enhances this activity.[15–18] However, the protocols used to derive these macrophages utilize supplements incompatible with therapeutic use in humans. Furthermore, because the therapeutic window for patients with infections is shorter than the time it takes to generate macrophages from CD14$^+$ blood monocytes (7 days), the cells must be produced in advance and cryopreserved to be available as an "off the shelf" therapy. Here we describe an approach to effectively modify the macrophage production process, with the goal of efficient, reproducible generation of cryopreserved human macrophages using therapeutically translatable xenobiotic-free (xeno-free) media (ICONIMAC™).

Generation and phenotypic characterization of GMP-compatible ICONIMAC™

To generate ICONIMAC™, purified CD14+ human peripheral blood monocytes were cultured in xeno-free, cGMP compatible base media supplemented with human macrophage colony-stimulating factor (60 ng/mL) to drive macrophage differentiation. On Day 6, cells were stimulated with IFNγ (20 ng/mL) to promote activation to an enhanced antimicrobial state and subsequently characterized. Because the process starts with positively-selected CD14+ cells and requires an extended culture period without other supportive cytokines, the product should not contain significant numbers of neutrophils, dendritic cells nor T and B cells whose presence could lead to GVHD.[19] Basic characterization of both fresh and cryopreserved ICONIMAC™ shows that these conditions result in a high cell yield (67.0% +/− 24% of input monocytes; 40 donors), as well as high viability (91.3% +/− 3.1%; 22 donors) and recovery (87.2% +/− 24%; 22 donors) post-thaw. Following differentiation, ICONIMAC™ morphology is consistent with canonical tissue culture-derived macrophages (Figure 1A; middle panel), and this morphology is maintained post cryopreservation (Figure 1A; right panel). ICONIMAC™ express macrophage differentiation marker CD206 (88.8% +/− 8.6%; Figure 1B) and upregulate M1 activation marker CD38 following stimulation with IFNγ (2.5-fold; Figure 1C). Broad unbiased profiling of 361 cell surface markers demonstrated that ICONIMAC™ is highly enriched for macrophage associated markers (CD206, CD163, CD64, CD14), macrophage activation markers (CD38, CD86), and displayed <1% of cell surface markers associated with a wide variety of other non-myeloid cell types, supporting the hypothesis that GVHD should not be an issue during clinical use (Figure 1D).

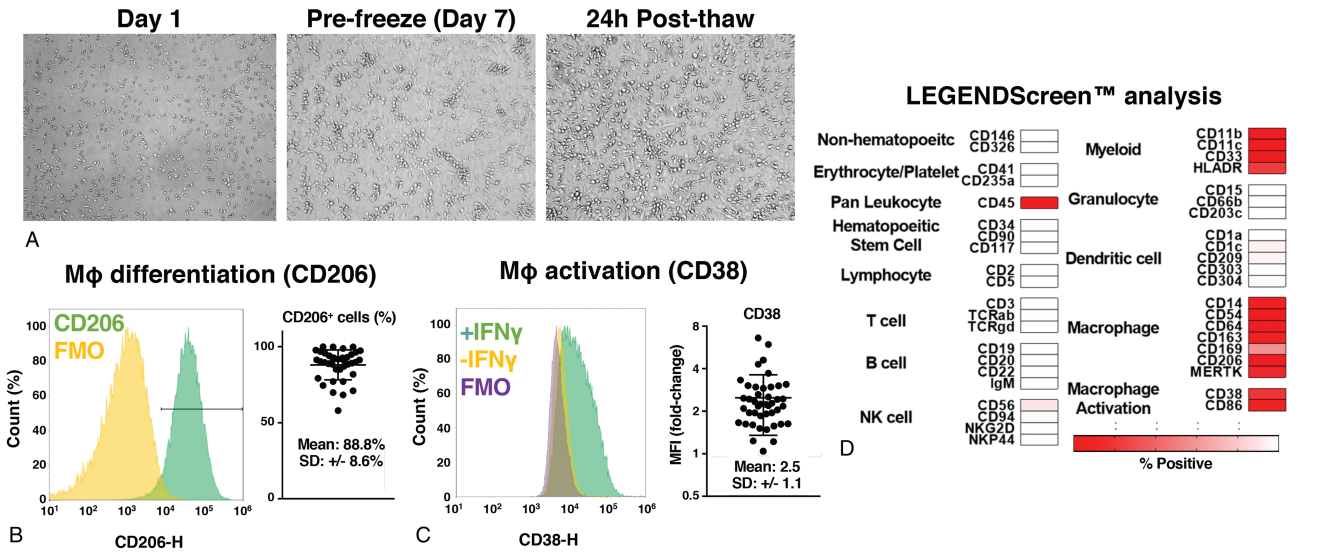

Figure 1. Phenotypic characterization of ICONIMAC™. A: Brightfield images of human peripheral blood-derived monocytes 1 and 7 days after selection and differentiation (left and middle panels), as well as images taken 24 h following cryopreservation (right panel). B: ICONIMAC™ surface marker expression analysis by flow cytometry. Left panel shows a representative histogram: CD206 (green) FMO control (orange). Right panel shows % of CD206+ cells across 38 donors. C: ICONIMAC™ expression of CD38 by flow cytometry. Left panel shows a representative histogram: IFNγ-treated (green), untreated (orange), FMO control (purple). Right panel shows fold induction of CD38 expression relative to untreated cells across 43 donors. D: Expression frequency of select surface markers as detected using LEGENDScreen™ (BioLegend) technology. Data from two donors mean value shown. FMO: fluorescence minus one; IFNγ: interferon-γ.

Functional characterization of ICONIMAC™

Analysis of a panel of cytokines and chemokines confirmed that ICONIMAC™ secretes proteins associated with macrophage activation including tumor necrosis factor-alpha (TNFα), interferon gamma-inducible protein 10 (IP-10), and RANTES (Figure 2A). Functional characterization showed that cryopreserved ICONIMAC™ readily internalized Gram-negative and Gram-positive bacteria (heat-killed *Staphylococcus aureus* or *Escherichia coli* labeled with a pH-dependent dye) and delivered them to acidic lysosomal compartments as shown qualitatively by microscopy (Figure 2B) and quantitatively by flow cytometry (Figure 2C). In these assays, actin polymerization inhibitor cytochalasin D served as a negative control, significantly reducing bacterial uptake. Consistent with the literature, ICONIMAC™ demonstrated a 2.0-fold induction of reactive oxygen species (ROS; Figure 2D) upon stimulation with phorbol 12-myristate 13-acetate (PMA), and an enhancement of glycolytic metabolism (1.5-fold at 120 minutes post-stimulation) as measured by the proton efflux rate (Figure 2E).

After the above basic characterization and functional validation of ICONIMAC™, the well-established gentamicin protection assay (GPA) was used to assess anti-bacterial efficacy of the cells in vitro. Standard microbiology minimum inhibitory concentration testing conducted on small molecule drugs to establish anti-bacterial efficacy is not technically feasible for ICONIMAC™; macrophages require complex tissue culture growth media and intimate contact with surrounding cells and matrix for optimal activity, and suspension turbidity readouts are not appropriate due to the turbidity generated by the presence of the cells themselves. For these reasons, researchers rely on functional assays such as the GPA to assess macrophage antimicrobial activity. Macrophages are exposed to bacteria to allow phagocytic uptake, at which point remaining extracellular bacteria are killed by exposing the culture to the cell-impermeable antibiotic gentamicin, and surviving intracellular bacterial colony-forming units (CFU) are enumerated immediately after antibiotic treatment ($t = 0$) and again after an additional 2 hours. ICONIMAC™ exhibited broad-spectrum activity against multidrug-resistant Gram-positive pathogens methicillin-resistant *S. aureus* and *Enterococcus faecium*, Gram-negative pathogen *Pseudomonas aeruginosa*, and carbapenem-resistant strains of Gram-negative *E. coli* or *Klebsiella pneumoniae*, each evidenced by a significant decline in surviving CFU 2 hours post-infection (Figure 2F).

Mouse bone marrow-derived macrophages (BMDM)-derived ICONIMAC™ as a surrogate in vitro efficacy test

To best model the treatment of infected patients with an adoptive antimicrobial "off the shelf" macrophage therapy, the cells must be derived from the same species as the model organism in which the infection is studied. To test ICONIMAC™ in vivo using established mouse infection models, we first generated a murine-derived ICONIMAC™ surrogate (Ms ICONIMAC™). Human ICONIMAC™ are differentiated from peripheral blood $CD14^+$ monocytes; however, given that an adult laboratory mouse reliably yields only ~1–1.5 mL of blood, generation of murine blood monocyte-derived macrophages was not feasible.[20] Bone marrow, which is rich in monocytes and monocyte precursors, has instead historically been used to generate sufficient quantities of primary murine macrophages for laboratory studies (BMDMs).[21] To generate Ms ICONIMAC™, murine bone marrow was cultured in

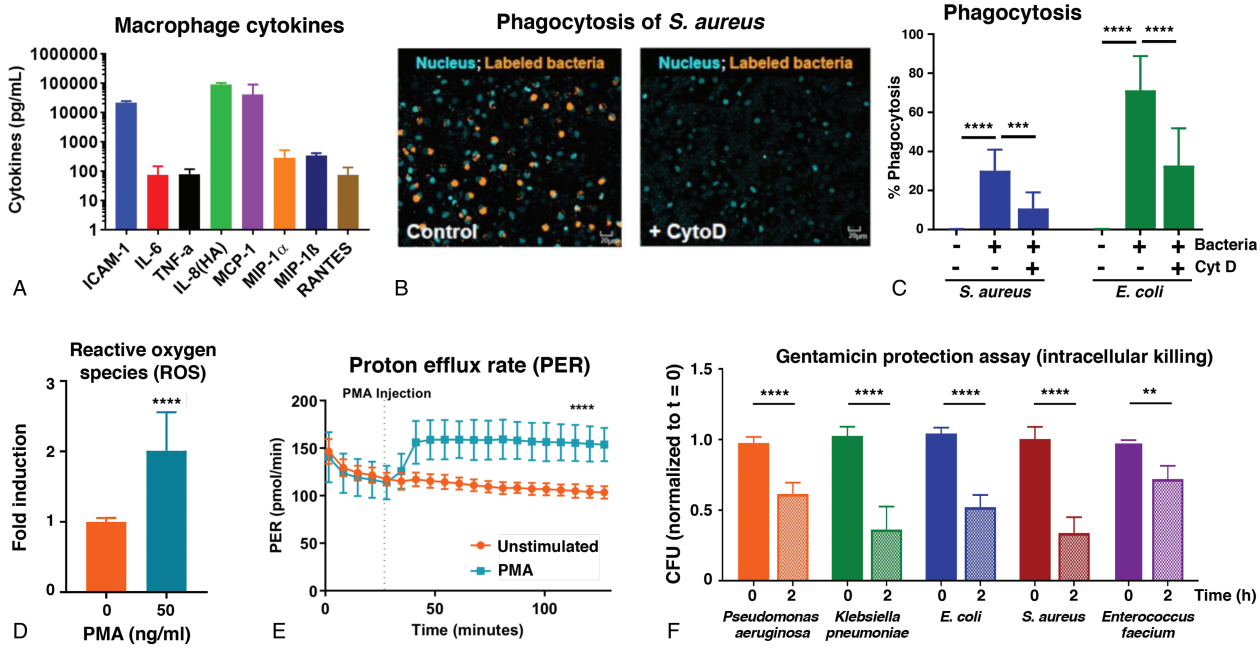

Figure 2. Functional characterization of ICONIMAC™. A: Cytokine levels from media collected on Day 7 of ICONIMAC™ differentiation and activation. B: Fluorescent microscopy of ICONIMAC™ (blue nuclei) treated with pHrodo-labeled *Staphylococcus aureus* (orange) for 2 h. Cytochalasin D (CytoD) used to inhibit phagocytosis. C: Phagocytosis of pHrodo-labeled *S. aureus* or *Escherichia coli* by ICONIMAC™ as detected by flow cytometry. Percent phagocytosis refers to the percentage of macrophages that positively stain for pHrodo dye indicating ingestion of the bacteria. Data from 12 donors; mean +/− SD. D: Detection of reactive oxygen species (ROS) induction by flow cytometry following 2 h PMA stimulation. Data from 46 donors; mean +/− SD. E: Proton efflux rate of ICONIMAC™ in presence or absence of PMA (50 ng/mL) was detected by Seahorse analysis over 120 min. Data from three donors mean +/− SD. F: Bacterial killing by ICONIMAC™ as assessed by gentamicin protection assay. Data from at least six donors; mean +/− SD. Statistical significances were assessed using *t*-test (D-F) and two-way ANOVA (B) ($^{**}P < 0.01$ $^{***}P < 0.001$, $^{****}P < 0.0001$). ANOVA: analysis of variance; PMA: phorbol 12-myristate 13-acetate; SD: standard deviation.

xeno-free, cGMP compatible base media supplemented with mouse macrophage colony-stimulating factor (60 ng/mL) to drive macrophage differentiation. On Day 6, cells were stimulated with mouse IFNγ (20 ng/mL) to promote enhanced antimicrobial activity. Morphologically, Ms ICONIMAC™ resembled standard BMDMs (Figure 3A). Phenotypic analysis revealed that the cells expressed myeloid marker CD11b (78.7%) and macrophage markers F4/80 and CD206 (76.6% double positive). Activation marker CD38 was also expressed (27.1%) on the differentiated and activated cells (Figure 3B). Functionally, Ms ICONIMAC™ upregulated ROS in response to PMA (1.7-fold; Figure 3C), phagocytosed pHrodo-labeled *S. aureus* as detected by flow cytometry (Figure 3D) and demonstrated intracellular killing of both *E. coli* and *S. aureus* in a GPA (Figure 3E). These data supported the use of Ms ICONIMAC™ derived from bone marrow as a reasonable mouse surrogate to study ICONIMAC™ efficacy in mouse infection models.

ICONIMAC™ improves survival outcomes in multidrug-resistant bacterial infection in vivo

To assess the direct and indirect antimicrobial mechanisms of adoptive macrophage therapy, allogeneic Ms ICONIMAC™ or human ICONIMAC™ were next tested in various in vivo peritoneal infection models using immunocompetent outbred hosts. Adult CD1 mice were infected *via* intraperitoneal injection with 4×10^8 CFU of methicillin-resistant *Staphylococcus aureus* (MRSA) (USA300 strain ATCC BAA-1717) or 2×10^8 CFU of a carbapenemase-producing *K. pneumoniae* strain (ATCC BAA-1705), with doses determined empirically to provide reliable 70%–90% lethality. Following infection, 1×10^6 ICONIMAC™ cells (allogeneic mouse or human) were administered intraperitoneally and survival was assessed over 7 days. In the Gram-negative *K. pneumoniae* infection model, meropenem (0.55 mg/kg) was given at a published effective murine dose as a SOC control, since this antibiotic is often used as a first line of empiric therapy in the clinic for peritonitis,[22] though not expected to be highly effective against the *K. pneumoniae* strain-producing strain. Whereas treatment with meropenem did not control infection, allogeneic (C57/BL6-derived) Ms ICONIMAC™ protected mice from *K. pneumoniae*-induced lethality ($P < 0.0001$; Figure 4A left panel). When Ms ICONIMAC™ was given in combination with meropenem, no change was observed in survival relative to Ms ICONIMAC™ alone, suggesting that the macrophage cell therapy can be implemented adjunctively to antibiotic therapy without sacrificing efficacy. Ms ICONIMAC™ at both high (1×10^6) and low (1×10^5) doses also conferred protection to CD1 outbred mice against MRSA-induced lethality ($P < 0.0001$ and $P < 0.01$, respectively; Figure 4A middle panel). Furthermore, Ms ICONIMAC™ provided protection against lethal lung infection with virulent *P. aeruginosa* strain PA01, showing that efficacy is not limited to the peritonitis model ($P < 0.0001$; Figure 4A right panel). Finally, human ICONIMAC™ also provided significant protection against mortality when thawed and administered adoptively in the murine MRSA peritonitis model ($P < 0.001$; Figure 4B).

ICONIMAC™ therapy reduces bacteria burden and improves systemic organ function

Analysis of CFU from the spleen and peritoneal lavage of MRSA-infected mice 6 hours post-infection and ICONIMAC™ administration revealed a 50.5% reduction in overall bacterial burden attributable to the macrophage cell therapy (Figure 5A). Importantly, analysis of serum from these mice showed that treatment with ICONIMAC™ mitigates infection-induced elevations in liver enzymes, suggesting a positive impact on limiting the progression to sepsis and a restoration of metabolic homeostasis (Figure 5B). To examine whether ICONIMAC™ therapy induces an enhanced antimicrobial state within the host, peritoneal lavage was collected 3 hours following MRSA infection and ICONIMAC™ administration and filtered to remove cells. The cell-free lavage was then diluted in bacterial growth media at the indicated dilutions and a growth assay was performed over 24 hours in a 37°C shaking incubator. A significant reduction ($P < 0.01$) in MRSA growth was seen in lavage fluid relative to phosphate-buffered saline (PBS)-treated control (Figure 5C), supporting the hypothesis that ICONIMAC™ orchestrates a broader anti-microbial response beyond direct killing. Together with the in vitro data, these findings show the therapeutic potential for ICONIMAC™ in treating drug-resistant bacterial infections.

The use of an allogeneic cell therapy raises potential concerns about immunological toxicity including GVHD and/or damaging inflammation secondary to host rejection of the graft.[23] As expected, ICONIMAC™ does not express lymphocyte markers (<1% by flow cytometry, Figure 1C), a characteristic critical for ensuring the product does not induce GVHD.[24] Detailed histopathology and standard clinical scoring parameters did

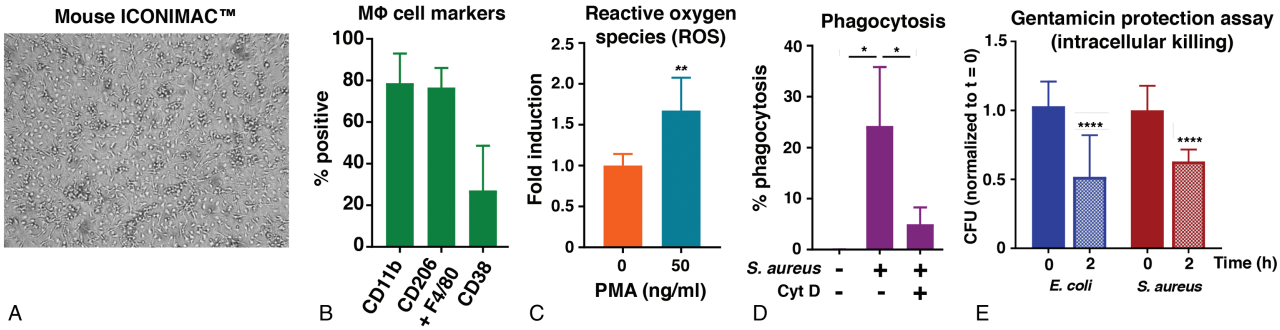

Figure 3. Characterization of Mouse ICONIMAC™. A: Brightfield image of mouse bone marrow-derived macrophages 7 days after isolation and differentiation. B: Surface marker expression of Ms ICONIMAC™ by flow cytometry. Data from four experiments; mean +/− SD. C: Detection of ROS induction by flow cytometry following 2 h PMA stimulation. Data from three experiments; mean +/− SD. D: Phagocytosis of pHrodo-labeled *Staphylococcus aureus* by Ms ICONIMAC™ as detected by flow cytometry. Data from three experiments; mean +/− SD. E: Bacterial killing by Ms ICONIMAC™ as assessed by gentamicin protection assay. Data from four experiments; mean +/− SD. Statistical significances were assessed using *t*-test ($^{*}P < 0.05$, $^{**}P < 0.01$, $^{****}P < 0.0001$). PMA: phorbol 12-myristate 13-acetate; ROS: reactive oxygen species.

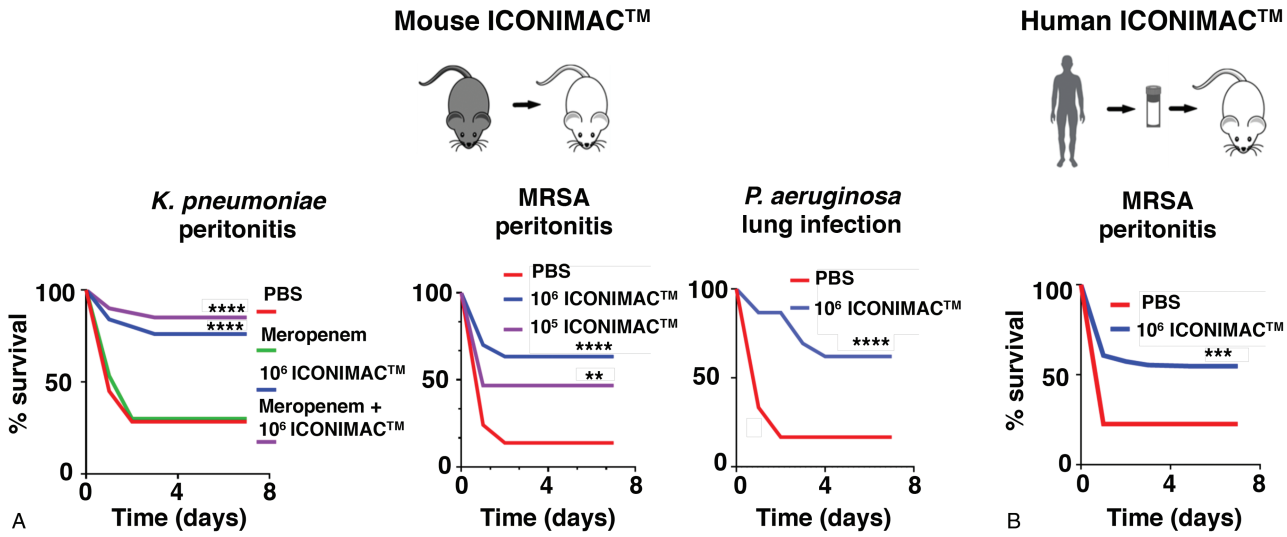

Figure 4. ICONIMAC™ in vivo efficacy. A: Survival of adult CD1 mice infected with *Klebsiella pneumoniae*, MRSA, or *Pseudomonas aeruginosa* and treated with antibiotics and/or Ms ICONIMAC™. Data from three experiments; ten mice per group per experiment. B: Survival of adult CD1 mice infected with MRSA and treated with human ICONIMAC™. Data from 15 experiments, one unique donor per experiment (15 donors total), ten mice per group per experiment. Statistical significances were assessed using log-rank Mantel-Cox test ($^{**}P<0.01$ $^{***}P<0.001$, $^{****}P<0.0001$). MRSA: methicillin-resistant staphylococcus aureus.

not reveal evidence of pathology in ICONIMAC™-treated mice in the 28-day observation period following ICONIMAC™ administration and bacterial clearance. Further, the immune cell landscape and proinflammatory cytokine milieu in the peritoneal lavage from infected and treated animals was not significantly altered by allogeneic mouse or human ICONIMAC™ therapy, consistent with an absence of inflammatory damage due to graft rejection (Figure 6). These findings are consistent with clinical data from allogeneic granulocyte transfusions in immunocompromised individuals (neutropenia or genetic leukocyte deficiencies) where frequency of proinflammatory cytokine storm was not significantly different than observed in untreated controls.[25]

Discussion

The ability to harness and enhance host immunity has been largely overlooked in treatment approaches to drug-resistant bacterial

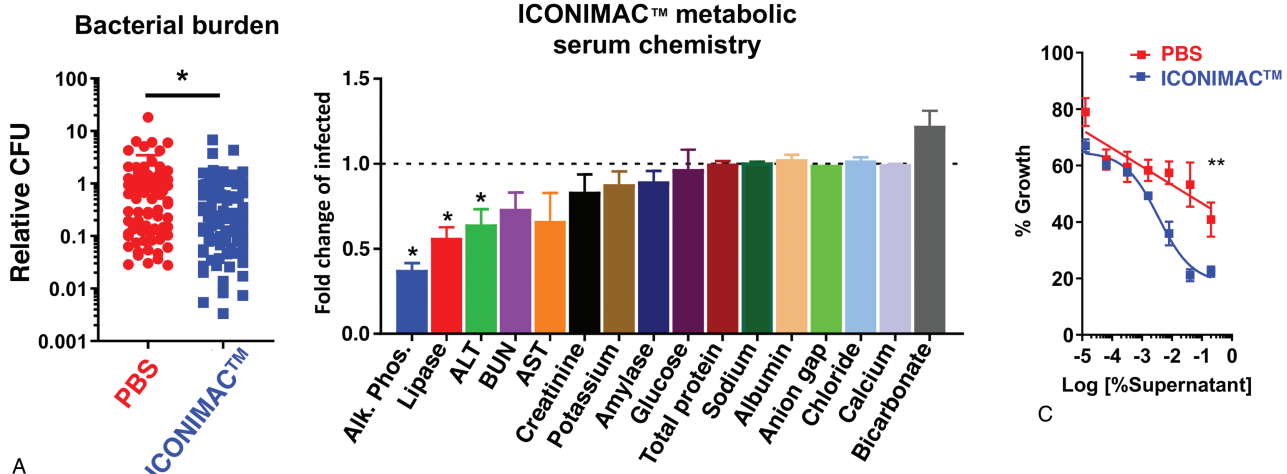

(U/L)	Alkaline Phosphatase	Lipase	ALT	AST
Reference	82 ± 21	N/A	29 ± 6	59 ± 9
Infection	551 ± 242	158 ± 127	73 ± 37	218 ± 93
ICONIMAC™	189 ± 71	78 ± 57	47 ± 18	152 ± 62

B

Figure 5. ICONIMAC™ therapy reduces bacterial burden and restores homeostasis. A: Normalized CFU of spleen and lavage fluid from mice infected with MRSA and treated with Ms ICONIMAC™. Each experiment was normalized to the mean of the PBS control for the corresponding tissue. Data from four experiments; ten mice per group per experiment. B: Analysis of metabolic markers from serum of mice 6 h following infection with MRSA and treatment with Ms ICONIMAC™. Data from three experiments; 25 mice per group total; mean +/− SD. C: MRSA growth assay in culture broth supplemented with the indicated ratio of cell-free peritoneal lavage fluid from MRSA-infected and Ms ICONIMAC™-treated mice. Data from three infected mice per group. Statistical significances were assessed using *t*-test (A and B) and two-way ANOVA (C) ($^{*}P<0.05$, $^{**}P<0.01$). ANOVA: analysis of variance; CFU: colony-forming units; MRSA: methicillin-resistant staphylococcus aureus; SD: standard deviation.

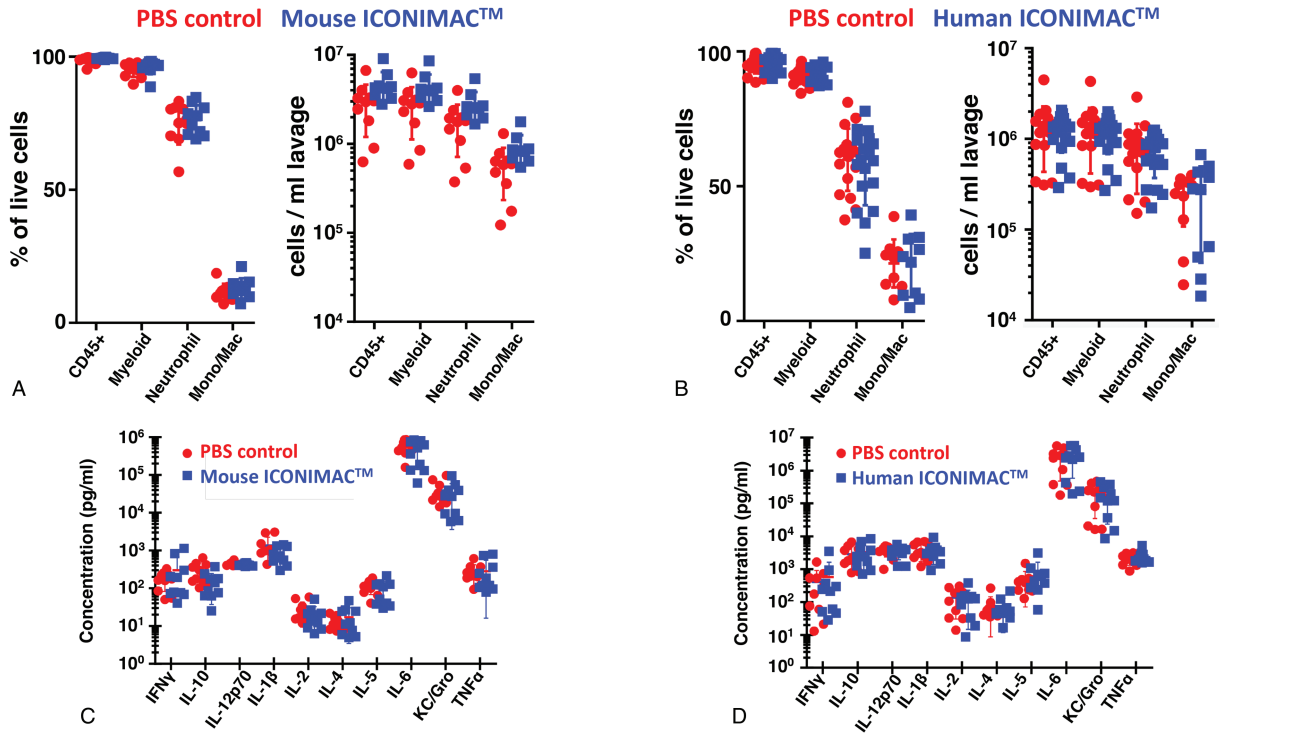

Figure 6. Inflammatory profile of ICONIMAC™-treated peritoneum. A and B: Flow cytometric analysis of peritoneal lavage of Ms ICONIMAC™ (A) and human ICONIMAC™ (B) treated mice 6 h following MRSA infection and treatment. Myeloid cells defined as CD45+CD11b+; neutrophils as CD45+CD11b+Ly6G+; Mono/Mac as CD45+CD11b+Ly6G-F4/80+. C and D: Cytokine analysis of peritoneal lavage collected 6 h following MRSA infection and treatment with Ms ICONIMAC™ (C) and human ICONIMAC™ (D). Data from ten mice per group and two unique human donors. MRSA: methicillin-resistant staphylococcus aureus.

infections. We hypothesized that acutely enhancing the broad MOA employed by the frontline effector cells of the innate immune system could serve as a powerful adjunct to antibiotic therapy. Macrophages are key orchestrators of innate immunity, with the ability to rapidly engulf and destroy pathogens, release soluble factors that attract and stimulate other immune cells, and ultimately restore baseline function.[8,9] Cell therapies that augment the immune response have dramatically improved clinical outcomes in oncology, but no one has yet similarly augmented the innate immune system for the acute treatment of bacterial infections.[26] In this report we show that ICONIMAC™, an allogeneic activated human macrophage cell therapy product, enhances survival of lethal bacterial infections and functions in concert with SOC (Figure 4). This novel approach confers three key potential advantages. First, macrophage cell therapy is expected to have a broad-spectrum of action. Considering that macrophages evolved to quickly defend the host against a diverse array of pathogens, this cell-based therapy should confer the necessary breadth of antimicrobial response to improve infection outcomes when combined with SOC, whether or not the organisms are resistant to pharmaceutical antibiotics. Second, macrophage cell therapy may have a lower propensity for resistance. Because healthy macrophages simultaneously deploy a wide array of effector mechanisms to exert their antimicrobial effects, it will be difficult for a single bacterial mutation to confer resistance to such multifaceted "combination therapy," thus suggesting a lower propensity for resistance, especially when used in conjunction with SOC. Finally, allogeneic macrophage cell therapy may have lower propensity for toxicity than other immunostimulatory strategies. By differentiating and activating macrophages outside of the body, this approach avoids the toxicities associated with systemic delivery of immune cell-activating agents such as IFNγ or GM-CSF. Because ICONIMAC™ is an allogeneic therapy, cells should be safely cleared within a week of delivery, decreasing any long-term risks seen with other types of cell therapies that expand and/or persist in the host. In addition, because ICONIMAC™ is a pure population of activated macrophages, it should avoid the GVHD risks that accompany cell-therapies comprising T or B cells.[19,27]

Previous work shows that therapeutic transfer of 4×10^6 human induced pluripotent stem cell (iPSC)-derived macrophages reduced disease-associated pathology and bacterial burden in a *P. aeruginosa* lung infection model.[28] However, their study utilized immunodeficient mice with impaired alveolar macrophage development (hIL3/GM-CSF KI mice) thus confounding their results.[29] Efficacy studies reported here using immune-competent mice show that dosing with 1×10^5 to 1×10^6 ICONIMAC™ per mouse largely rescues mice from Gram-negative and Gram-positive bacterial-induced lethality in models of peritonitis and lung infection (Figure 4). When extrapolated to a 70 kg adult human, this dose roughly equates to 1×10^8 to 2×10^9 cells per dose, comfortably within the expected yield of monocyte-derived macrophages from a leukopak preparation of apheresed healthy donor blood.[30–32]

Previously, human clinical studies were conducted using autologous monocyte-derived macrophages *via* multiple routes of administration including intravenously, intraperitoneally (IP), and intravesicularly.[30,31] These trials demonstrated that despite the high number of cells delivered (up to 10^9 cells per dose), the therapy was relatively safe and well-tolerated, with the majority of reported side effects being minor fever/chills without serious adverse events.[30] These clinical studies also tracked radioisotope-labeled macrophages and showed that cells delivered IP were retained in the peritoneal cavity for 5–7 days, with minimal signal detected in the bloodstream and no signal detected in other organs.[33] Generation of the autologous product is very similar to that

proposed for ICONIMAC™, thus we hypothesize that the distribution of cells will be similar in ICONIMAC™ therapy. However, because ICONIMAC™ is an allogeneic therapy, more studies are needed in the future to understand toxicity, distribution and residence time. Interestingly, analysis of the peritoneal lavage of infected mice following Ms or human ICONIMAC™ treatment shows no change in proinflammatory cytokine production nor immune cell infiltration, suggesting that ICONIMAC™ therapy does not induce damage to the host due to excessive inflammation (Figure 6). While the lack of a significant increase in macrophages present in the peritoneal lavage of mice treated with murine ICONIMAC™ is surprising, it is possible that the subtle difference in mean macrophage numbers 569,337 and 905,727 in the phosphate-buffered saline (PBS) and ICONIMAC™ groups respectively reflect an expected, albeit inefficient, recovery of adoptively transferred cells (Figure 6A). Additionally, activated macrophages are not readily released into the peritoneal lavage due to integrin-mediated adherence to the peritoneal lining *via* a physiologic phenomenon termed the "macrophage disappearing reaction."[34] Observations of treated mice over 28 days supports our claim that ICONIMAC™ therapy is not harmful to the host as no evidence of pathology was detected.

Macrophages limit bacteria insult *via* several MOAs including direct phagocytosis and bacterial killing, release of extracellular factors that induce bacterial killing, and recruitment/activation of neighboring immune cells to orchestrate a robust immune response. ICONIMAC™ therapy both reduces the overall bacterial burden of infected mice in a model of peritonitis (Figure 5A) and renders the peritoneum less hospitable to bacterial growth (Figure 5C). Interestingly, evidence of immune orchestration was not readily apparent, as inflammatory cytokine production and immune cell composition of the peritoneum were unchanged following therapy (Figure 6). These data suggest that the primary mechanism for ICONIMAC™-mediated rescue of peritonitis-induced mortality is phagocytosis and/or the induction of an anti-microbial state that limits the pathology associated with infection. Macrophages are also critically important in restoration of damaged tissue following infectious or inflammatory insult. We observe that liver enzymes present in the serum following infection were significantly reduced (Figure 5B), suggesting that ICONIMAC™ therapy may also contribute to restoration of tissue homeostasis.

In summary we have developed a macrophage-based cell therapy that demonstrates the following key parameters for a successful anti-microbial cell therapy strategy: (i) a simple, short, and GMP-compatible differentiation process (7 days, Figure 1); (ii) a pure macrophage population with durability following cryopreservation (Figure 1), (iii) an allogeneic cell therapy product that does not induce hyperinflammation nor GVHD (Figure 6); and (iv) an efficacious dose that falls in line with a reasonable expected yield from a donor leukopak (1×10^9 cells in humanized dosing; Figure 4). These data support the continued exploration of an allogenic macrophage-based cell therapy as an adjunctive strategy to treat intractable bacterial infections.

Methods

Isolation of monocytes from peripheral blood and generation of monocyte-derived macrophages

Peripheral blood mononuclear cells were isolated from human blood using both Ficoll-Paque (GE Healthcare, Chicago, IL, USA) and Leucosep tubes (Greiner Bio-One, Monroe, NC, USA) by density gradient centrifugation. $CD14^+$ cells were positively selected by CD14 Microbeads and MS MACS Columns (Miltenyi Biotec, San Diego, CA, USA). $CD14^+$ cells were differentiated for 7 days in 100 mm dishes (Ultra-Low Attachment dishes, Corning, Corning, NY, USA) at $1.5–2.0 \times 10^6$ cells/mL. M0 macrophages were cultured in DendriMACS GMP Medium (Miltenyi Biotec, San Diego, CA, USA), media supplemented with 1X Glutamax and 120 ng/mL M-CSF (Biolegend, San Diego, CA, USA). Fresh M-CSF added every 2–3 days, and on day 6 M0 cells were activated with 20 ng/mL IFNɣ (Biolegend, San Diego, CA, USA). M1 macrophages were harvested on Day 7 with a non-enzymatic cell dissociation solution (CellStripper Dissociation Reagent, Corning, Corning, NY, USA) and cryopreserved in GMP grade, animal-free freezing medium (Stem-CellBanker, Ambsbio LLC, Abingdon, UK) at $5.0 \times 1\ 0^6$ cells/mL.

Generation of bone marrow-derived macrophages

Bone marrow from the femur and tibia of C57BL/6 mice was isolated by centrifugation through a needle punctured micro-centrifuge tube. Bone marrow cells were differentiated for 7 days in 100 mm dishes at $1.5–2.0 \times 10^6$ cells/mL. M0 macrophages were cultured in Roswell Park Memorial Institute (RPMI)-1640 (Corning), media supplemented with 10% fetal bovine serum (FBS), 1X Glutamax, and 60 ng/mL Mouse M-CSF (Biolegend, San Diego, CA, USA). Fresh mouse M-CSF added every 2–3 days, and on Day 6 M0 cells were activated with 20 ng/mL mouse IFNγ (Biolegend, San Diego, CA, USA). M1 macrophages were harvested on Day 7 with a non-enzymatic cell dissociation solution (CellStripper Dissociation Reagent, Corning, Corning, NY, USA).

Flow cytometry

For cell surface staining, 50,000 cells per condition were placed in Cell Staining Buffer (Biolegend). Mouse TruStain FcX or human True-Stain Monocyte Blocker (BioLegend, San DIego, CA, USA) was added at 1:25 to block Fc receptors and incubated for 10 minutes on ice in the dark. Human samples were stained at a dilution of 1:10 with CD38 (HIT2) and CD206 (15–2) and fluorescence minus one controls. Mouse samples were stained at a dilution of 1:200 with CD11b (M1/70), CD206 (C068C2), F4/80 (BM8), and CD38 (90). All samples were also stained with Zombie NIR dye (Biolegend) at 1:1000 for live/dead gating. All antibodies were sourced from Biolegend. Samples were incubated with antibody cocktail for 20 minutes in the dark on ice. After antibody incubation cells were washed with buffer and fixed in 4% paraformaldehyde for 20 min in the dark on ice. Samples were washed again and resuspended in fresh buffer then ran on a NovoCyte Flow Cytometer (Acea Bioscience, San Diego, CA, USA). Flow cytometric analysis was performed using NovoExpress software (Acea Bioscience, San Diego, CA, USA). LEGENDScreen (BioLegend, San Diego, CA, USA) staining and analysis performed per manufacturer's instructions. For flow-cytometric analysis of the peritoneum, 3 mL of PBS was injected into the peritoneal cavity and subsequently retrieved. This procedure was repeated three times. Cellularity of the lavage was determined, and the lavage fluid was subsequently centrifuged. Pelleted cells were then stained with antibodies and run on a flow cytometer as described above. For analysis of cytokines within the peritoneum, supernatant from only the first wash was isolated and assessed.

Cytokine detection

Cell culture supernatant or peritoneal lavage fluid (PLF) was collected, and cells were eliminated by centrifugation. Super-

natants were then assessed for cytokine concentration using Meso QuickPlex SQ 120 (Meso Scale Discovery, Rockville, MD, USA) per manufacturer's instructions. Peritoneal lavage was assessed using V-Plex Pro-Inflammatory Kit II (Meso Scale Discoveries, Rockville, MD, USA). Cell culture supernatant was assessed using V-Plex Human Biomarker Kit (Meso Scale Discovery, Rockville, MD, USA).

Phagocytosis assay

Fifty thousand cells were plated in 96-well round bottom plates and resuspend in Live Imaging Solution (Invitrogen, Carlsbad, CA, USA) with Hoechst stain (NucBlue Reagent, Invitrogen, Carlsbad, CA, USA). A control group was treated with cytochalasin D (50 μg/mL) at 37°C for 10 minutes. pHrodo particles (pHrodo Red *S. aureus* or *E. coli* BioParticles, Invitrogen, Carlsbad, CA, USA) were prepared by adding 2 mL Live Imaging Solution to each vial of particles, followed by gently mixing; 10 μL of pHrodo particles was then added per well. Cells and particles were incubated at 37°C for 120 minutes and samples run on a NovoCyte Flow Cytometer (Acea Bioscience, San Diego, CA, USA) collecting. Flow cytometric analysis was performed using NovoExpress software (Acea Bioscience, San Diego, CA, USA).

ROS induction assay

Fifty thousand cells per well were plated into 96-well round bottom plates in complete medium with 20 μM DCFA (Cellular ROS Assay Kit, abCam, Cambridge, UK). Cells were incubated at 37°C for 30 minutes, then DCFA was removed and replaced with fresh media with 50 ng/mL PMA. Cells were incubated for 3 hours and then run on a NovoCyte Flow Cytometer (Acea Bioscience, San Diego, CA, 92130).

Glycolytic induction assay

Twenty-five thousand cells were plated in eight well Seahorse Xp chamber and cultured overnight. Cells were stimulated with 50 ng/mL and assessed on Seahorse XFp Extracellular Flux Analyzer for 2 hours. Induction of glycolysis was determined by measurement of proton efflux rate.

Gentamicin protection assay

One lakh cells per well were plated into a 96-well plate in complete media without antibiotics and incubated overnight. Overnight cultures of bacteria were diluted and grown to $OD_{600} = 0.4$ (ATCC, *P. aeruginosa* BAA-211, *K. pneumoniae* BAA-1705, *E. coli* BAA-2340, MRSA BAA-1717, *E. faecium* BAA-2316; all strains purchased from ATCC). Bacteria were aliquoted for cell inoculation (multiplicity of infection 20 or 2×10^6 CFU/well) and added to washed cells in complete media devoid of antibiotics. The plate was centrifuged at 3000 rpm for 5 minutes, then incubated at room temperature for 5 minutes. Next, the plates were washed with 100 μL/well PBS, and 100 μL of RPMI with 10% FBS and 100 μg/mL gentamicin added to kill unengulfed bacteria. Plates were incubated at 37°C and 5% CO_2 for 30 minutes, then washed ×2 with 200 μL/well PBS. For time 0 ($T = 0$), cells were lysed with 0.025% TritonX, incubated at room temperature for 10 minutes, and lysates serially diluted and plated onto Luria broth (LB) agar plates. Remaining cells were cultured for 2 hours in gentamicin free media, then lysed with 0.025% TritonX, incubated at room temperature for 10 minutes, and lysates serially diluted and plated onto LB agar plates. Colonies were counted and CFU calculated relative to $T = 0$.

In vivo infection models. Peritonitis

Cultures of MRSA (ATCC BAA-1717) or *K. pneumoniae* (ATCC BAA-1705) were thawed and cultured until log-phase growth achieved. Bacteria were suspended in PBS (100 μL/mouse) at 4×10^8 CFU for MRSA and 2×10^8 CFU for *K. pneumoniae*. Bacteria were injected IP into female CD1 mice (10–12 weeks old), followed immediately by IP injection of indicated doses of Hu or Ms ICONIMAC™ suspended in 100 μL PBS. Survival was assessed daily. For studies assessing bacterial burden, peritoneal lavage, spleen, and blood were harvested from euthanized mice 6 hours post infection. The spleen was dissociated using TissueLyser II (Qiagen, Germantown, MD, USA) and the resulting homogenate, as well as the peritoneal lavage, were serially diluted and plated on LB-agar plates to determine CFU. Serum was isolated from collected blood samples and a comprehensive serum metabolic panel was obtained from the UC San Diego Murine Hematology and Coagulation Core Laboratory. CFU were calculated relative to the median CFU of the control group per tissue per experiment. Bacterial burden was then defined as the sum of the relative CFUs from peritoneum and spleen.

Lung infection

Mice were anesthetized with ketamine/midazolam IP, inoculated intratracheally with 1×10^7 CFU PAO1, followed by intratracheal administration of 1×10^7 ICONIMAC™. Survival was assessed over a 7-day period, and moribund mice euthanized by CO_2 asphyxiation. The UC San Diego Institutional Animal Care and Use Committee approved all animal use and procedures.

Ex vivo bacterial killing assay

Female outbred CD1 mice (8–12 weeks old) were challenged by IP injection with or without 4×10^8 MRSA, followed by subsequent administration of ICONIMAC™ treatment. One hour post-treatment, mice were euthanized by CO_2 asphyxiation and PLF collected using 3 mL of chilled (4°C) RPMI. PLF was collected through a 0.2 μm membrane and in a 96-well format, minimum inhibitory concentration broth dilution (1:5) in RPMI + 10% Todd-Hewitt broth was performed. Samples were incubated for 24 h and absorbance 600 nm was determined.

References

[1] Centers for Disease Control and Prevention. Antibiotic Resistance Threats in the United States. 2019. Available from: https://www.cdc.gov/drugresistance/pdf/threats-report/2019-ar-threats-report-508.pdf. Accessed November 25, 2019.
[2] Burnham JP, Olsen MA, Kollef MH. Re-estimating annual deaths due to multidrug-resistant organism infections. Infect Control Hosp Epidemiol 2019;40(1):112–113.
[3] Vincent JL, Rello J, Marshall J, et al. International study of the prevalence and outcomes of infection in intensive care units. JAMA 2009;302 (21):2323–2329.
[4] Fernandes P, Martens E. Antibiotics in late clinical development. Biochem Pharmacol 2017;133:152–163.
[5] Linehan E, Fitzgerald DC. Ageing and the immune system: focus on macrophages. Eur J Microbiol Immunol (Bp) 2015;5(1):14–24.
[6] Shaw AC, Goldstein DR, Montgomery RR. Age-dependent dysregulation of innate immunity. Nat Rev Immunol 2013;13(12):875–887.

[7] Sarantis H, Grinstein S. Subversion of phagocytosis for pathogen survival. Cell Host Microbe 2012;12(4):419–431.
[8] Martinez FO, Sica A, Mantovani A, Locati M. Macrophage activation and polarization. Front Biosci 2008;13:453–461.
[9] Murray PJ, Wynn TA. Protective and pathogenic functions of macrophage subsets. Nat Rev Immunol 2011;11(11):723–737.
[10] Baquir B, Lemaire S, Van Bambeke F, Tulkens PM, Lin L, Spellberg B. Macrophage killing of bacterial and fungal pathogens is not inhibited by intense intracellular accumulation of the lipoglycopeptide antibiotic oritavancin. Clin Infect Dis 2012;54(Suppl 3):S229–S232.
[11] Czyż DM, Jain-Gupta N, Shuman HA, Crosson S. A dual-targeting approach to inhibit Brucella abortus replication in human cells. Sci Rep 2016;6:35835.
[12] Czyz DM, Potluri LP, Jain-Gupta N, et al. Host-directed antimicrobial drugs with broad-spectrum efficacy against intracellular bacterial pathogens. MBio 2014;5(4):e01534-14.
[13] Mosser DM, Edwards JP. Exploring the full spectrum of macrophage activation. Nat Rev Immunol 2008;8(12):958–969.
[14] Price JV, Vance RE. The macrophage paradox. Immunity 2014;41 (5):685–693.
[15] Weiss G, Schaible UE. Macrophage defense mechanisms against intracellular bacteria. Immunol Rev 2015;264(1):182–203.
[16] Sechler JM, Malech HL, White CJ, Gallin JI. Recombinant human interferon-gamma reconstitutes defective phagocyte function in patients with chronic granulomatous disease of childhood. Proc Natl Acad Sci USA 1988;85(13):4874–4878.
[17] Borden EC, Sen GC, Uze G, et al. Interferons at age 50: past, current and future impact on biomedicine. Nat Rev Drug Discov 2007;6(12):975–990.
[18] Borden EC. Augmentation of effects of interferon-stimulated genes by reversal of epigenetic silencing: potential application to melanoma. Cytokine Growth Factor Rev 2007;18(5–6):491–501.
[19] Sale GE. Pathogenesis of graft-versus-host-disease. Biol Blood Marrow Transplant 2005;11(2 Suppl 2):21–23.
[20] Diehl KH, Hull R, Morton D, et al. European Federation of Pharmaceutical Industries, European Centre for the Validation of Alternative MethodsA good practice guide to the administration of substances and removal of blood, including routes and volumes. J Appl Toxicol 2001;21(1):15–23.
[21] Manzanero S. Generation of mouse bone marrow-derived macrophages. Methods Mol Biol 2012;844:177–181.
[22] de Fijter CW, Jakulj L, Amiri F, Zandvliet A, Franssen E. Intraperitoneal meropenem for polymicrobial peritoneal dialysis-related peritonitis. Perit Dial Int 2016;36(5):572–573.
[23] Porter DL, Antin JH. Graft-versus-leukemia effect of allogeneic bone marrow transplantation and donor mononuclear cell infusions. Cancer Treat Res 1997;77:57–85.
[24] Choi SW, Levine JE, Ferrara JL. Pathogenesis and management of graft-versus-host disease. Immunol Allergy Clin North Am 2010;30(1):75–101.
[25] Price TH, Boeckh M, Harrison RW, et al. Efficacy of transfusion with granulocytes from G-CSF/dexamethasone-treated donors in neutropenic patients with infection. Blood 2015;126(18):2153–2161.
[26] Guedan S, Ruella M, June CH. Emerging cellular therapies for cancer. Annu Rev Immunol 2019;37:145–171.
[27] Sarantopoulos S, Blazar BR, Cutler C, Ritz J. B cells in chronic graft-versus-host disease. Biol Blood Marrow Transplant 2015;21(1):16–23.
[28] Ackermann M, Kempf H, Hetzel M, et al. Bioreactor-based mass production of human iPSC-derived macrophages enables immunotherapies against bacterial airway infections. Nat Commun 2018;9(1):5088.
[29] Willinger T, Rongvaux A, Takizawa H, et al. Human IL-3/GM-CSF knock-in mice support human alveolar macrophage development and human immune responses in the lung. Proc Natl Acad Sci USA 2011;108 (6):2390–2395.
[30] Lee S, Kivimae S, Dolor A, Szoka FC. Macrophage-based cell therapies: the long and winding road. J Control Release 2016;240:527–540.
[31] Fraser AR, Pass C, Burgoyne P, et al. Development, functional characterization and validation of methodology for GMP-compliant manufacture of phagocytic macrophages: a novel cellular therapeutic for liver cirrhosis. Cytotherapy 2017;19(9):1113–1124.
[32] Svensson A, Adamson L, Pisa P, Petersson M, Hansson M. Monocyte enriched apheresis for preparation of dendritic cells (DC) to be used in cellular therapy. Transfus Apher Sci 2005;33(2):165–173.
[33] Ritchie D, Mileshkin L, Wall D, et al. In vivo tracking of macrophage activated killer cells to sites of metastatic ovarian carcinoma. Cancer Immunol Immunother 2007;56(2):155–163.
[34] Barth MW, Hendrzak JA, Melnicoff MJ, Morahan PS. Review of the macrophage disappearance reaction. J Leukoc Biol 1995;57(3):361–367.